PubMed Central CANADA

Author Manuscript / Manuscrit d'auteur

Nat Neurosci. Author manuscript; available in PMC 2016 August 04.

Published in final edited form as:

Nat Neurosci. 2013 February ; 16(2): 183–192. doi:10.1038/nn.3295.

Morphine hyperalgesia gated through microglia-mediated disruption of neuronal Cl^- homeostasis

Francesco Ferrini[1,2,3,*], **Tuan Trang**[4,5,6,*], **Theresa-Alexandra M. Mattioli**[6], **Sophie Laffray**[1,2], **Thomas Del'Guidice**[1,2], **Louis-Etienne Lorenzo**[1,2], **Annie Castonguay**[1,2], **Nicolas Doyon**[1,2], **Wenbo Zhang**[4,5], **Antoine G. Godin**[1], **Daniela Mohr**[4,5], **Simon Beggs**[4,5], **Karen Vandal**[‡,1], **Jean-Martin Beaulieu**[1,2], **Catherine Cahill**[7], **Michael W. Salter**[4,5], and **Yves De Koninck**[1,2]

[1]Institut Universitaire de santé mentale de Québec, Québec, G1J 2G3, Canada

[2]Department of Psychiatry and Neuroscience, Université Laval, Québec, Québec, G13 7P4, Canada

[3]Department of Veterinary Sciences, University of Turin, 10095, Grugliasco, Turin, Italy

[4]Program in Neurosciences & Mental Health, Hospital for Sick Children, Toronto, Ontario, M5G 1X8, Canada

[5]Department of Physiology, University of Toronto, Toronto, Ontario, Canada

[6]Departments of Comparative Biology & Experimental Medicine, and Physiology & Pharmacology, Hotchkiss Brain Institute, University of Calgary, Calgary, Canada

[7]Department of Pharmacology & Toxicology, Queen's University, Kingston, Ontario, Canada

Abstract

A major unresolved issue in treating pain is the paradoxical hyperalgesia produced by the gold-standard analgesic morphine and other opiates. We show here that hyperalgesia-inducing treatment with morphine causes downregulation of the K^+-Cl^- cotransporter KCC2, impairing Cl^- homeostasis in spinal lamina l neurons. Restoring E_{anion} reversed the morphine-induced hyperalgesia without affecting tolerance. The hyperalgesia was also reversed by ablating spinal microglia. Morphine hyperalgesia, but not tolerance, required μ opioid receptor-dependent expression of P2X4 receptors (P2X4Rs) in microglia and μ-independent gating of the release of

Please send correspondence to: Yves De Koninck, Division of Cellular and Molecular Neuroscience, Institut universitaire de santé mentale de Québec, 2601, Chemin de la Canardière, Québec, QC, G1J 2G3, CANADA, Phone: 418-663-5747 ext. 6885, FAX: 418-948-9030, Yves.DeKoninck@crulrg.ulaval.ca.

*These authors contributed equally to this work

‡This paper is dedicated to the memory of Karen Vandal who passed away during the course of this study.

AUTHOR CONTRIBUTIONS

F.F., T.T., C.C., M.W.S., Y.D.K. conceived and designed the project. C.C., J.M.B.,.Y.D.K., M.W.S. supervised the experiments. F.F., T.T., T.-A.M.M., S.L., T.D.G., L-E.L., A.C., W.Z., D.M., K.V. performed the experiments. N.D. performed computer simulations and contributed to interpretation of results. S.B. generated CD11b-Cre+/LoxBDNF mice. F.F., T.T., T.-A.M.M., S.L., T.D.G., L-E.L., A.C., N.D., W.Z., A.G.G. analyzed the data. F.F., T.T., M.W.S. and Y.D.K. wrote the manuscript. All authors read and discussed the manuscript.

COMPETING FINANCIAL INTERESTS

The authors declare no competing financial interests.

brain-derived neurotrophic factor (BDNF) by P2X4Rs. Blocking BDNF-TrkB signalling preserved Cl^- homeostasis and reversed the hyperalgesia. Gene-targeted mice in which BDNF was deleted from microglia did not develop hyperalgesia to morphine. Yet, neither morphine antinociception nor tolerance was affected in these animals. Our findings dissociate morphine-induced hyperalgesia from tolerance and unveil the microglia-to-neuron P2X4-BDNF-KCC2 pathway as a therapeutic target to prevent hyperalgesia without affecting morphine analgesia.

Morphine, and other opiates, are indispensable in the treatment of moderate to severe postoperative and chronic pain, but use of these drugs is plagued by the development of two major problems: tolerance and hyperalgesia[1]. Tolerance is characterized by a progressive lack of response to morphine that can be overcome by increasing the dose, while hyperalgesia is a sensitization process in which opioids, paradoxically, cause pain hypersensitivity[2]. Commonly-held views are that tolerance and hyperalgesia reflect a single underlying cellular and molecular mechanism[3,4].

The spinal dorsal horn (SDH) of the spinal cord is a main site of action for the analgesic effects of morphine and other opiates, and has been implicated in morphine-induced hyperalgesia (MIH) and tolerance[5,6]. Within the SDH nociceptive information is received from sensory fibers, processed and relayed to brain areas involved in mediating the sensory and emotional aspects of pain[7]. Nociceptive processing involves neuron-neuron and neuron-glia interactions through multiple facilitatory and inhibitory signaling cascades regulating the final output of the pain signaling networks. But how morphine acts on these networks in the SDH to produce hyperalgesia or tolerance remains enigmatic.

In the SDH, lamina I (L_I) neurons comprise one of the principal output pathways to the brain[8–10]. These neurons are central targets for opioid analgesia[5], which inhibit their activity. Conversely, increasing the output in this pathway is implicated as a neuronal substrate underlying morphine tolerance and hyperalgesia[6,9]. Spinal nociceptive output is not only increased by enhanced excitation but also by diminished inhibition[10] and the latter has recently been implicated as a substrate of several chronic pain conditions[11]. Although morphine causes analgesia via inhibition in the SDH, here we set out to explore the seemingly counterintuitive concept that morphine may also cause disinhibition, the latter being the neuronal substrate for hyperalgesia and/or tolerance.

We show that morphine induced hyperalgesia via a P2X4R-BDNF-KCC2 disinhibition cascade between microglia and SDH neurons. Interfering with the principal nodes in the cascade suppresses hyperalgesia but has no effect on tolerance. The disinhibition resulted from impaired Cl^- extrusion in L_I neurons. Pharmacological blockade of P2X4Rs reversed hyperalgesia and mouse lacking these receptors did not develop hyperalgesia. Similarly hyperalgesia was reversed by blocking BDNF-TrkB signaling and did not develop in mice lacking BDNF in microglia. Finally, restoring hyperpolarizing inhibition reversed morphine hyperalgesia. Our findings thus define the signaling pathway underlying MIH, opening avenues to specifically prevent this highly deleterious effect of morphine without affecting its analgesic action.

Results

To determine whether there is a common or separate mechanism for tolerance and hyperalgesia, we used a differential testing paradigm in rats treated with morphine sulphate (10 mg/kg subcutaneous) twice daily over 7 days. Morphine antinociception was measured by testing thermal withdrawal threshold 1 h after each morning injection ($n = 14$; $P < 0.001$; Fig. 1a). While morphine induced a significant increase in thermal withdrawal threshold at that time point on day 1, the antinociception was significantly reduced within 3 days of treatment ($P < 0.001$; Fig. 1a). By day 5, morphine had no effect on withdrawal threshold, indicating that the animals were tolerant to antinociceptive effects of morphine. Development of hyperalgesia was assessed separately by testing animals just prior to each morning injection of morphine (Fig. 1b–c). We found a progressive decrease in withdrawal threshold over the course of 5–7 days of morphine treatment ($n = 14$; $P < 0.001$), but not with saline injections ($n = 10$; $P > 0.05$; Fig. 1b–c), indicating the development of pain hypersensitivity in these animals. Pain hypersensitivity was also shown by increased responses to nociceptive stimulation: vocalizations in response to the subcutaneous injections ($n = 7$; $P < 0.05$; Fig. 1d) and licking behaviour after thermal stimulation ($n = 7$; day 7, $P < 0.05$; Fig. 1e) were increased by repeated morphine treatment. In contrast, no change in motor performance was observed using the accelerating rotarod test (Fig. 1f) indicating that the decrease in withdrawal thresholds was not due to altered motor activity. That the time course for the development of hyperalgesia is different from tolerance raised the possibility of distinct underlying mechanisms.

MIH is due to altered Cl^- homeostasis

Disinhibition through disrupting Cl^- homeostasis is one mechanisms for increasing the output of L_I neurons in the SDH[12,13]. Therefore, we investigated whether morphine caused altered Cl^- homeostasis in L_I neurons. We measured Cl^- extrusion capacity of these neurons in spinal cord slices isolated from rats receiving either saline or morphine injections for 7 days (Fig. 2a–b)[14]. Upon applying an intracellular Cl^- load we found that E_{GABA} in morphine-treated rats (-42.3 ± 1.3 mV, $n = 6$) was significantly more depolarized compared to saline-treated rats (-50.1 ± 2.2 mV, $n = 5$; $P < 0.05$; Fig. 2d). Because hyperalgesia may also develop within hours of high dose treatments[15], we incubated spinal cord slices from naïve rats with 1 μM morphine for 3 h. *In vitro* morphine also caused a significant shift in E_{GABA} (control $n = 6$; morphine $n = 12$; $P < 0.01$; Fig. 2c–d). Thus, both repeated and high-dose morphine treatment impair Cl^- extrusion in L_I neurons.

To separately test whether morphine weakens Cl^- extrusion, we used an established paradigm involving collapse of the Cl^- gradient during trains of evoked inhibitory postsynaptic currents (eIPSCs)[16]. The contribution of Cl^- accumulation to activity-dependent depression of synaptic activity was determined by stimulating inhibitory transmission while holding the membrane potential either above (0 mV) or below (−90 mV) E_{Cl}[16]. When holding at −90 mV the rate of decrease of eIPSC amplitude depends on activity-dependent synaptic depression, whereas at 0 mV the rate of decrease reflects synaptic depression plus postsynaptic Cl^- accumulation[16]. Morphine did not affect the rate of synaptic depression at −90 mV (Fig. 2e; $P > 0.05$), consistent with the lack of presynaptic

μreceptor expression in spinal inhibitory interneurons[17]. In contrast, the decrease in eIPSC amplitude at 0 mV was faster after morphine (Fig. 2f; CTR: $n = 6$; MS: $n = 4$; $P < 0.05$). The differential effect of morphine at 0 mV *vs* −90 mV indicates that morphine caused increased Cl^- accumulation. Thus, morphine weakened Cl^- extrusion as measured with Cl^- loaded either tonically through the patch pipette or phasically through synaptic receptors.

Further evidence of a collapse in Cl^- gradient in neurons exposed to morphine was found in the responses to exogenous GABA applied in presence of physiological $[Cl^-]_i$ in cells held near the resting potential (−60 mV; Fig. 2g). In these neurons GABA evoked a biphasic response – an initial outward current followed by a shift to an inward current (Fig. 2g) as previously described in neurons with impaired Cl^- extrusion capacity[14,18]. In contrast, in L_I neurons not exposed to morphine, the response to GABA remained outward at − 60 mV (Fig. 2g). The inward component of the response to GABA has been associated with outward flux of HCO_3^- becoming predominant when the Cl^- gradient collapses, yielding a progressive depolarizing shift in E_{GABA}[14,19,20]. To determine whether this was the case in neurons exposed to morphine, we bath-applied acetazolamide (ACTZ, 50 μM), a cell-permeant inhibitor of carbonic anhydrase, the enzyme responsible for generating HCO_3^- intracellularly[20]. In the presence of ACTZ the GABA response remained outward, yielding a 10 mV hyperpolarizing shift in E_{GABA}, measured 1 s after the onset of the GABA puff (Fig. 2g). These findings are consistent with ACTZ lowering the generation of HCO_3^- resulting in an activity-dependent depletion of HCO_3^-, and ensuing loss of HCO_3^- efflux, during the GABA response[20] (supplementary Fig. 1).

Preventing the progressive shift in E_{GABA} in neurons with impaired Cl^- extrusion has been found to substantially restore inhibition[19,21]. Thus, ACTZ may mitigate the impact of the morphine-induced collapse in Cl^- gradient, rescuing the impairment of inhibition. We therefore tested the effects of intrathecal administration of ACTZ in rats with established hyperalgesia after 7–9 days of morphine-treatment. ACTZ administration reversed morphine-induced mechanical and thermal hypersensitivity (Fig. 2h). We conclude that ACTZ reversed the hyperalgesia by reducing HCO_3^--mediated inward current thereby restoring E_{GABA}. Taken together, our findings indicate that altered anion homeostasis underlies MIH.

Morphine reduces Cl^- transport and KCC2 expression

In adult L_I neurons, Cl^- homeostasis is mainly regulated by the K^+-Cl^- cotransporter, KCC2[12,22]. We therefore determined the effect of repeated morphine treatment on spinal KCC2 expression. After 7 days of morphine treatment there was a significant decrease in KCC2 immunoreactivity in L_I of morphine-treated ($n = 5$, 103.4 ± 5.8, intensity units – i.u.) as compared with saline treated rats ($n = 5$, 191.2 ± 5.8 i.u.; $P < 0.01$; Fig. 3a). Concordantly, KCC2 protein levels in SDH homogenates were reduced by morphine (Fig. 3b). As KCC2 oligomerization may be critical for transporter function[23], we analyzed the KCC2 oligomer/monomer ratio in the absence of detergents and found that the ratio was significantly reduced in the SDH of morphine-treated rats ($n = 8$ control; $n = 9$ morphine-treated rats; $P < 0.05$; Fig. 3c). In contrast, morphine had no effect on KCC2 expression or oligomer/monomer ratio in the spinal ventral horn (Fig. 3b–c). Thus, the morphine-induced

impairment in Cl^- homeostasis in L_I neurons may result from loss of the oligomeric form of KCC2 in these cells.

To test whether total KCC2 activity in L_I neurons is affected by morphine, we examined the transporter activity in reverse mode[24] by measuring K^+-driven uptake of Cl^-. We performed intracellular Cl^- imaging and stepped extracellular K^+ from 2.5 mM to 15 mM in control or morphine-treated slices (1μM for 3 h) (Fig. 3d–e). The rate of Cl^- accumulation was significantly slower in morphine-treated neurons ($n = 8$, 0.32 ± 0.04 (%ΔF/F)/s) than in controls ($n = 8$, 0.54±0.2 (%ΔF/F)/s, $P < 0.05$; Fig. 3e). These data indicate that morphine impairs Cl^- homeostasis by reducing KCC2-mediated Cl^- transport.

MIH, but not tolerance, requires spinal microglia

Because microglia have been implicated in disrupting Cl^- homeostasis in L_I neurons[22,25] we questioned whether MIH may differentially depend upon spinal microglia. We found that repeated morphine induced an increase in immunoreactivity for CD11b, which is specifically expressed by microglia in the CNS (Fig. 4a), indicating that spinal microglia respond to morphine treatment. To determine whether spinal microglia are required for morphine tolerance or hyperalgesia, we depleted microglia in the spinal cord of morphine-treated rats using intrathecal injection of a saporin-conjugated anti-mac1 antibody[26] (Fig. 4b). Intrathecal injections were begun at day 7, when both pain hypersensitivity and morphine tolerance had been established. Within 2 days, saporin-conjugated anti-mac1 (20–36 μg), but not saporin alone (20 μg), reversed morphine-induced thermal pain hypersensitivity ($n = 6$ saporin-treated and $n = 7$ anti-mac1 saporin-treated; $P < 0.01$; Fig. 4c). Saporin-conjugated anti-mac1 also reversed morphine-induced mechanical allodynia (mechanical threshold at day 7 of morphine injection: 0.4 ± 0.1 of the baseline, $n = 5$; mechanical threshold at day 8 of morphine injection following intrathecal anti-mac-1 saporin administration: 1.2 ± 0.3 of the baseline, $n = 5$; $P < 0.05$). In contrast, saporin-conjugated anti-mac1 had no effect on morphine tolerance ($P > 0.05$; Fig. 4d). Thus, we conclude that microglia in the SDH are necessary for the ongoing expression of hyperalgesia but not for tolerance caused by repeated morphine treatment.

To determine whether morphine-treated microglia are sufficient to produce pain hypersensitivity we used an *in vivo* microglia transfer approach[22,27]. Microglia in primary culture were chronically treated with morphine and then injected intrathecally at the lumbar spinal level in naïve rats (Fig. 5a). We found that mechanical withdrawal threshold was markedly decreased after intrathecal administration of morphine-treated microglia ($n = 7$; $P < 0.001$; Fig. 5a). By contrast, mechanical withdrawal threshold was unaffected by saline-treated microglia. Thus, morphine-treated microglia are sufficient to cause pain hypersensitivity in naïve animals.

Microglial P2X4 receptors are required for MIH

Pain hypersensitivity produced by microglia critically depends on P2X4 receptors (P2X4Rs) [27] suggesting that morphine-induced pain hypersensitivity may require microglial P2X4Rs. We found that the decrease in withdrawal threshold produced by transferring morphine-treated microglia was prevented by TNP-ATP, an antagonist at P2X1,2,3,4Rs, but

not by PPADS, an antagonist at P2X1,2,3,5,7Rs[27], implicating P2X4Rs in the expression of the pain hypersensitivity evoked by morphine-treated microglia (Fig. 5a). Moreover, we found that repeated morphine treatment caused no change in thermal and mechanical withdrawal threshold, licking time or vocalization in *P2rx4* null mutant mice (*P2rx4*$^{-/-}$; Fig. 5b–d) but *P2rx4*$^{+/+}$ mice developed multiple signs of pain hypersensitivity in response to morphine (Fig. 5b–d). Thus, P2X4Rs are required for the development of hyperalgesia. To test whether P2X4Rs are also necessary for the ongoing expression of hyperalgesia we administered TNP-ATP (30 nmol) intrathecally in morphine-treated animals. We found that TNP-ATP reversed the decrease in thermal withdrawal threshold that had developed after 7 days of morphine (Fig. 5e), without affecting morphine tolerance (Fig. 5f). In another series of experiments, intrathecal TNP-ATP also reversed established mechanical allodynia in morphine-treated rats (Fig. 5g).

As our findings indicate that P2X4Rs are required for the development and ongoing expression of hyperalgesia caused by morphine we questioned whether morphine treatment may increase expression of P2X4Rs, which is normally at a low level in the naïve CNS[27,28]. In the *P2rx4*$^{-/-}$mice, where the *P2rx4* gene was replaced with *lac z*, we found a greater X-gal signal in the spinal cord of morphine- than in saline-treated animals (Fig. 5h). Moreover, we found that repeated morphine treatment increased P2X4R protein in wild type animals (illustrated below). To determine whether morphine may act directly on microglia we used primary microglia cultures and found that chronic morphine treatment caused an increase in P2X4R protein level (Fig. 5i). These receptors were functional as indicated by morphine-induced increase in P2X4R-mediated currents (Fig. 5j) and Ca^{2+} responses (see below). Thus, MIH depended upon P2X4Rs, and morphine caused an increase in *P2rx4* gene expression autonomously in microglia.

MIH, but not tolerance, requires microglial BDNF

Stimulation of P2X4Rs in microglia evokes release of brain derived neurotrophic factor (BDNF)[22,29,30] known to downregulate KCC2 expression in adult neurons[31]. Therefore, we wondered whether morphine may cause a P2X4R-dependent release of BDNF from microglia. We found that after chronic treatment, morphine caused release of BDNF from primary microglia cultures (Fig. 6a). The morphine-evoked release of BDNF was blocked by TNP-ATP but unaffected by PPADS (Fig. 6a). BDNF release was also blocked by the ATP-degrading enzyme apyrase (Fig. 6a), indicating that morphine causes release of BDNF through ATP-mediated stimulation of P2X4Rs. The mechanical hypersensitivity evoked by morphine-treated microglia was prevented by a BDNF-sequestering fusion protein (TrkB-Fc)[32], but not by the control peptide IgG-Fc (Fig. 6b). Altogether our findings indicate that morphine causes P2X4R-dependent release of BDNF from microglia which is sufficient to cause pain hypersensitivity.

We then addressed whether BDNF, and signaling through its cognate receptor TrkB, is necessary for morphine-induced impairment in Cl^- extrusion capacity of L_I neurons and ensuing hyperalgesia. The shift in E_{GABA} induced by morphine treatment was prevented by co-incubation with the function blocking anti-TrkB antibody (Fig. 6c–d). To determine whether BDNF-TrkB signaling is required for the ongoing expression of MIH, we tested the

effects of intrathecal injections of the anti-TrkB antibody. Anti-TrkB produced a gradual reversal of thermal hyperalgesia over 3 days in rats treated with morphine for 7 days, comparable to that obtained by ACTZ treatment (see above and Fig. 6e); however, neither anti-TrkB nor ACTZ affected morphine antinociception (Fig. 6f), indicating that BDNF and associated disrupted Cl^- homeostasis are required for ongoing expression of MIH, but not tolerance.

To determine whether the requisite BDNF is released from microglia we used gene-targeted mice in which BDNF was deleted in microglia. These mice were generated by crossing animals expressing Cre recombinase under the control of the CD11b promoter (CD11b-Cre^+) with those in which exon 5 of the BDNF gene, that encodes the BDNF protein, was flanked by LoxP sites (LoxBDNF) yielding CD11b-Cre^+/LoxBDNF mice[33,34]. Lumbar spinal activity of the CD11b-Cre transgene was verified by crossing mice with Rosa26 mice that ubiquitously express the β-galactosidase (β-Gal) transgene[33]. Microglia, but not neurons or astrocytes, expressed β-gal in Rosa26/CD11b-Cre^+ mice. In addition, Cre expression was detected only in cells that stained for the microglial markers iba-1 and CD11b (Beggs et al., in preparation). No differences in mechanical nociceptive behaviour were observed between CD11b-Cre^+/LoxBDNF mice (1.5 ± 0.2 g, n=7) and their littermate LoxBDNF controls (1.5 ± 0.2 g, n=7; P>0.05). However, only LoxBDNF mice developed robust hyperalgesia upon repeated morphine, whereas no change in mechanical withdrawal threshold, licking time, or vocalization was found in CD11b-Cre^+/LoxBDNF (Fig. 7a–c). CD11b-Cre^+/LoxBDNF mice and LoxBDNF mice were indistinguishable in the following parameters: peak antinociceptive response to a single dose of morphine (Fig. 7d); progressive increase in ED50 to escalating morphine doses; shift in the morphine dose-response curve following 5 days of morphine treatment (Fig. 7e); and expression of naloxone-precipitated signs of withdrawal (Fig. 7f). Thus, acute morphine antinociception, tolerance and withdrawal behavior were not altered in the CD11b-Cre^+/LoxBDNF mice. We conclude that BDNF specifically from microglia is required for the hyperalgesia induced by morphine.

Both μ-dependent and μ-independent signaling are necessary

The simplest cascade of events accounting for our findings is that the hyperalgesia induced by morphine is driven by increased expression of P2X4Rs in microglia leading to release of BDNF that acts through TrkB receptors to downregulate functional expression of KCC2 with subsequent disruption of Cl^- homeostasis in L_I neurons. This raises the question of what are the direct molecular targets of morphine and their location, or locations, in this core pathway. The direct molecular target for morphine-induced analgesia are the well-known seven transmembrane isoforms of the μ opioid receptor[35]. Expression of μ receptors is evident in spinal microglia[36] (supplementary Fig. 2). On the other hand, there is increasing evidence that the actions of morphine or its metabolites may be dependent on concurrent activation of μ receptor-independent pathways[37,38]. To interrogate the possible requirement for the latter we examined the effects of stereoisomers of the opioid receptor antagonist naloxone: (−)naloxone blocks both μ-and non-μ-mediated signaling; (+)naloxone blocks only the non-μ-mediated mechanisms[37]. We found that spinally administered (+)naloxone prevented morphine hyperalgesia (Fig. 8a) but did not affect the development of tolerance (Fig. 8b). Moreover, (+)naloxone significantly reduced morphine-induced upregulation of

CD11b (Fig. 8c) and prevented the shift in E_{GABA} in L_I neurons in spinal slices treated with morphine ($n = 8$; $P > 0.05$; Fig. 8d). Finally, (+)naloxone precluded the hyperalgesic action of intrathecal administration of morphine-treated microglia (Fig. 8e). Thus, μ receptor-independent signaling is essential for the microglia-neuron interactions that cause hyperalgesia.

To examine whether morphine targets specifically in microglia, we tested naloxone stereoisomers in the cultured microglia that are competent to transfer hyperalgesia. Morphine-induced increases in P2X4R expression and function in microglia cultures were blocked by (−)naloxone but were unaffected by (+)naloxone (Fig. 8f–g). Similarly, the increase in spinal P2X4R expression caused by repeated morphine administration *in vivo* was prevented by (−)-naloxone but not by (+)naloxone (Fig. 8h). The morphine-induced increase in microglial P2X4Rs therefore required μ opioid receptors. However, and surprisingly, morphine-evoked release of BDNF in microglia cultures with already upregulated P2X4R expression, was prevented by (+)-naloxone (Fig. 8i). Thus, we conclude that, in microglia, μ receptors mediate the upregulation of P2X4Rs and a μ receptor-independent mechanism is required for the morphine-stimulated release of BDNF.

The mechanisms of μ receptor-independent signaling by morphine are not fully understood. It has been suggested that toll-like receptors 4 (TLR4) mediate morphine-induced neuroinflammatory responses[39]. To test the potential involvement of TLR4 we measured morphine-induced release of BDNF from microglia cultures in the presence of the TLR4 antagonist LPS-RS[39]. Across a range of concentrations, LPS-RS had no effect on morphine-induced release of BDNF (Fig. 8j), consistent with our previous finding that LPS treatment does not induce BDNF release from microglia[29]. In addition, here we found that mice lacking functional TLR4 (C3H/HeJ) developed tactile hypersensitivity with morphine treatment that was indistinguishable from that of wild type controls (C3H/HeOuJ; Fig. 8k). These findings indicate that TLR4 is not required for morphine hyperalgesia.

Discussion

Our findings define the core pathway by which morphine produces hyperalgesia, ultimately through dysregulation of Cl^- homeostasis in pain-signaling neurons in spinal L_I. The most parsimonious interpretation is that this pathway is initiated by morphine acting on μ opioid receptors in SDH microglia which, through release of BDNF, signal to the L_I neurons causing the Cl^- dysregulation by driving down expression of KCC2. Although, like hyperalgesia, morphine tolerance is dependent upon μ receptors[40], our results demonstrate that microglia and the subsequent components of the hyperalgesia pathway are not required for tolerance. That hyperalgesia and tolerance are mechanistically distinct is consistent not only with the observation that tolerance and hyperalgesia have differing clinical characteristics[41], but also with recent findings uncovering the signaling pathways underlying morphine tolerance, which do not affect hyperalgesia[42]. Our results also indicate that the mechanism we uncovered represents a substrate of ongoing hyperalgesia induced by morphine rather than withdrawal hyperalgesia.

A key concept emerging from our findings is that morphine causes disinhibition by disrupting neuronal Cl^- homeostasis. Yet, morphine is thought of as causing inhibition either pre- or postsynaptically. Thus, morphine-induced spinal disinhibition is a new paradigm for actions of this drug and other opiates. We show that, in the SDH, this disinhibition leads to the paradoxical hyperalgesic action of morphine. A therapeutic avenue that follows from this finding to prevent or reverse selectively the hyperalgesia is to restore $GABA_A$ and/or glycine receptor-mediated inhibition, achieved by enhancing $GABA_A$ receptor activation through positive modulation such as with benzodiazepines[43]. This strategy may be of limited efficacy however given our finding that disinhibition results from dysregulation of Cl^- homeostasis. Indeed, if E_{GABA} is depolarized beyond a certain point, enhancing $GABA_A$ transmission may become counterproductive[21]. In such condition, restoring E_{GABA} by blocking the carbonic anhydrase to attenuate the depolarizing HCO_3^- component of $GABA_A$/glycine-mediated currents is a potential approach to reverse morphine hyperalgesia, as it has been done to improve the antihyperalgesic potency of benzodiazepines[44]. Activity-dependent accumulation of Cl^- through $GABA_A$ or glycine channels resulting from compromised Cl^- extrusion capacity will nevertheless provoke some breakdown of inhibition with the above approaches[19]. Thus, ultimately, restoring Cl^- extrusion capacity through enhancing KCC2 expression or activity[31] will likely be more effective as an adjuvant therapy to chronic morphine treatment.

Disinhibition and hyperalgesia caused by morphine were mediated by upregulation of P2X4Rs in the spinal cord microglia *in vivo,* driving synthesis and release of BDNF[29,30]. Morphine has been found to upregulate P2X4Rs[45] and to induce BDNF transcription[46] via μ receptors in microglia *in vitro*. These findings point to a role for μ receptor activation in the microglia signaling cascade leading to hyperalgesia. Yet, our results reveal unexpectedly that, while μ receptor activation causes P2X4R upregulation, μ receptor-independent signaling is necessary for the subsequent BDNF release. Unlike suggested previously[39], our results do not support an involvement of TLR4 in this mechanism. This apparent discrepancy may be due to the much lower doses of morphine used in the present study, although more work is needed to define the underlying pharmacology. P2X4R-dependent as well as μ receptor-independent pathways represent strategic targets for the pharmacological prevention of MIH, as their activation can be blocked without interfering with μ receptor-mediated analgesia[37].

Our results also reveal that the spinal disinhibition underlying MIH results from BDNF-TrkB signaling[47]. Inflammatory and neuropathic pain also depend on BDNF-TrkB signaling. Yet, in inflammatory pain BDNF arises from primary afferents[48], whereas neuropathic pain hypersensitivity depends upon BDNF from microglia[22,30]. In both MIH and neuropathic pain the synthesis and release of BDNF from microglia requires P2X4R upregulation[29,30] in contrast to inflammatory pain. Our results thus demonstrate that MIH shares a common aetiology with neuropathic pain.

Our results establish a unexpected commonality in mechanisms between MIH, pain hypersensitivity after peripheral nerve injury[22] and the sequelae of spinal cord injury[49]. Altered Cl^- homeostasis, by causing depolarizing $GABA_A$-mediated events, may also contribute to NMDA receptor plasticity[12,25], thus favoring the onset of opioid-induced LTP

in spinal neurons[9]. Moreover, our findings may extend to mechanisms involved in morphine-induced drug dependence in critical reward centers of the brain. For example, BDNF causes a switch from $GABA_A$-mediated inhibition to excitation –suggestive of altered Cl^- homeostasis– in the ventral tegmental area in opiate-dependent rats[50]. Neuronal dysfunction in the mesolimbic reward pathways is considered a key mechanism underlying addiction. Thus, our discovery may provide a new perspective on drug dependence, as involving cross talk between microglia and neurons leading to neuronal disinhibition in key brain regions that underlie reward and addiction.

Morphine hyperalgesia can no longer be seen as an inevitable consequence of morphine analgesia or tolerance. Of particular importance to therapeutic development, we show that continuous activation of this signaling pathway is necessary to specifically maintain MIH, while it has no effect on tolerance or withdrawal signs. We demonstrate that it is possible to reverse what causes the established pain hypersensitivity, potentially alleviating opiate use liability. Importantly, this can be accomplished by targeting non-classical opioid receptors or by restoring Cl^- homeostasis in SDH neurons, sparing morphine analgesia mechanisms. Taken together, our findings and the recent demonstration of a distinct mechanism underlying morphine tolerance[42] overturn the traditional dogma of the common mechanism underlying both morphine tolerance and hyperalgesia, and establish a basis for a novel approach to enhance the utility of morphine in treating chronic pain.

METHODS

Animals

Adult male mice and rats (>P60) were used. Animals were housed under 12:12 h light/dark cycle. All experimental procedures have been performed in accordance with guidelines from the Canadian Council on Animal Care.

Chronic morphine protocol and behavioural models

Morphine sulphate (morphine, Sandoz, QC, Canada) was injected twice a day (9 a.m. and 6 p.m.) in Sprague–Dawley rats (10 mg/Kg), *P2rx4*$^{+/+}$ or *P2rx4*$^{-/-}$ C57BL/6 mice (Dr. Rassendren[51], INSERM, France; escalating doses from 10 to 40 mg/Kg), CD11b-Cre$^+$/LoxBDNF or LoxBDNF mice (escalating doses from 10 to 40 mg/Kg), C3H/HeOuJ (TLR4 wild type) or C3H/HeJ (functionally deficient TLR4 mutant) mice (escalating doses from 10 to 40 mg/Kg; Jackson lab., ME, USA[52]). Morphine was injected subcutaneously, unless otherwise stated. Thermal pain threshold was measured by Hargreaves plantar test prior to and 1 h after morphine injection. Morphine antinociceptive effect measured 1 h after injection in chronically treated animals is not explained by altered metabolism[53]. Mechanical pain threshold was measured prior to morphine injection by von Frey hairs, as described[12]. Values are normalized to the control. Vocalizations were monitored during subcutaneous injections and differences in the relative number of vocalizing rats (%) or in the number of vocalizations (in mice) were analysed. Licking time was measured during thermal or mechanical stimulation of the hind-paw. Motor coordination was measured by accelerating rotarod (IITC Life Science, CA, USA) prior to and 30, 60 min after morphine injections. In a subset of experiments, a morphine cumulative dose-response curve was

performed on day 6 to determine morphine ED50 value. Briefly, animals were given ascending doses of morphine every 30 min and the response to morphine was assessed by the thermal tail-flick test until a maximal level of antinociception was reached. In all behavioural studies, experimenters were blind to the drug treatments and genetic profile of the animal.

Behavioural assessment of naloxone-precipitated withdrawal

Mice received intraperitoneally ascending doses of systemic morphine at 8 h intervals (day 1: 10 and 20 mg/kg; day 2: 25, 30 mg/kg; day 3: 35, 40 mg/kg; and day 4: 45, 50 mg/kg). On day 5, animals received a morning injection of 55 mg/kg and 2 h later naloxone (2 mg/kg) to precipitate withdrawal. Control animals received saline and were challenged with naloxone on day 5. Animals were acclimatized to a clear Plexiglass testing chamber 1 h prior to naloxone. Signs of withdrawal were compiled as previously described[54]. Briefly, jumping, headshakes, wet-dog shakes, and grooming behavior were evaluated at 10 min intervals for a total testing period of 30 min and a standardized score of 0 to 3 was assigned (0 = absent; 1 = 1–3 bouts; 2 = 4–6 bouts, and 3 = 7 bouts and greater). Paw tremors, piloerection, salivation, and ejaculation were also evaluated with one point being given to the presence of each sign during each 10 min interval. The number of periods showing the latter signs were then counted (maximum score of 3 per behavioural sign) and the scores added together to yield a final cumulative withdrawal score. Animals were also weighed before and after naloxone challenge and weight loss (an indicator of micturition and defecation) was calculated.

Generation of CD11b-Cre^{+}/LoxBDNF mice

Mice with microglial-lineage specific excision of BDNF were generated using the Cre-lox system. C57BL/6J mice, heterozygous for CD11b-Cre were purchased from the European Mutant Mouse Archive (provided by George Kollias, Alexander Fleming Biomedical Research Center, Vari, Greece)[33]. 129S4/SvJae mice homozygous for floxed BDNF (Bdnf^{tm3Jae}/J) were purchased from Jackson (stock 00439). These mice express *loxP* sites flanking exon 5 of the BDNF gene[34]. Homozygous Bdnf^{tm3Jae}/J mice were crossed with heterozygous CD11b-Cre mice and Cre expressing progeny back-crossed with homozygous Bdnf^{tm3Jae}/J mice to ensure all experimental animals were homozygous for Bdnf^{tm3Jae}/J and matched for background strains. Mice were genotyped by PCR analysis. CD11b-Cre^{+}/LoxBDNF mice exhibit normal nociceptive responses under control conditions.

Intrathecal injections

In a subset of experiments (where indicated), rats were subject to drug administration via intrathecal catheters. Rats were anaesthetized with 4% isoflurane and a catheter was inserted into the intrathecal space as described[55]. Unless otherwise stated, intrathecal injections were delivered 30 min prior to subcutaneous morphine or saline injections. Animals were tested 20 min after intrathecal injection (immediately prior to morphine or saline injection) and 1 h later. At the end of the experiment, the correct placement of the catheter was verified. Drugs included saporin (20 μg) and saporin-conjugated anti-mac-1 (16–32 μg; Advanced Targeting Systems, CA, USA), anti-TrkB (30 μg; R&D Systems, MN, USA), acetazolamide (22.5 μg; Sigma, MO, USA), TNP-ATP (2′,3′-O-(2,4,6-trinitrophenyl)adenosine 5′-triphosphate, 30

nmol; Tocris, MT, USA), naloxone (5 ng; Sigma, MO), (+)-naloxone (5 ng; Dr. Evans, NIDA). All drugs were dissolved in a HEPES-buffered ringer (pH 7.8).

Spinal cord slice preparation

Parasagittal slices (300 μm) of the spinal cord were prepared, as described[12]. Slices were allowed to recover for 1 h in artificial cerebrospinal fluid (ASCF) containing (in mM): 126 NaCl, 2.5 KCl, 2 $MgCl_2$, 2 $CaCl_2$, 1.25 NaH_2PO_4, 26 $NaHCO_3$, 10 glucose.

Patch-clamp recordings from L_I neurons

Voltage clamp recordings were performed as described[12]. The following intrapipette solutions were used: for whole cell experiments involving measurements of E_{GABA} under Cl^- load, (in mM): 115 K-methylsulfate, 25 mM KCl, 2 $MgCl_2$, 10 HEPES, 4 ATPNa, 0.4 GTPNa, 0.1% Lucifer Yellow (LY), pH 7.2; for whole cell experiments to study evoked IPSCs, (in mM): 135 K-methylsulfate, 5 mM KCl, 0.5 EGTA, and the rest as above; for perforated patch-clamp recordings: 115 K-methylsulfate, 25 mM KCl, 2 $MgCl_2$, 10 HEPES, 0.1% Lucifer Yellow (LY), 30 μg/ml gramicidin (Sigma), pH 7.2. Membrane potential measurements were corrected for liquid junction potential. Data were filtered at 5 kHz, digitized and acquired using the Strathclyde electrophysiology software (Dr. J. Dempster, University of Strathclyde, UK). GABA (1 mM) was puffed locally for 30 ms. The puff pipette was aimed toward the center of the neuronal somata, approximately 5 μm away from the recording pipette. Experimental E_{GABA} was extrapolated from the $GABA_A$ I-V relationships. The difference between the experimental and the theoretical E_{GABA} (according to Hodgkin-Katz-Goldman equation) provides an estimate of Cl^- extrusion capacity as described[14]. Recordings of repeated eIPSCs were performed in the presence of bath-applied CNQX (10 μM) and APV (40 μM). IPSCs were evoked by focal electrical stimulation (100 μA, 200 μs). Trains of stimuli (25 pulses - 20Hz) were delivered every 20 s at 0 or −90 mV. Ten consecutive trains were averaged for subsequent analysis. In electrophysiological experiments, only neurons with resting membrane potential < −50 mV and stable access resistance were included for subsequent analysis. No differences in access resistance were observed between morphine-treated (19.3±0.9 MΩ) and untreated neurons (20.2±1.1 MΩ). At the end of each recording session a photograph of the recorded neuron was acquired. Data analysis was performed off-line with Clampfit 10.2 (Molecular Devices).

Imaging of reverse Cl^- transport in L_I neurons

Slices were labelled in ACSF containing 5 mM of the Cl^- indicator MQAE (N-6-methoxyquinolinium acetoethylester; Molecular Probes) and 0.2% pluronic in DMSO (Sigma) for 40–45 minutes at RT. Slices were then transferred to a perfusion chamber (2 ml/min) and extracellular MQAE was washed out for 30 minutes in the presence of (in μM): 1 TTX, 10 CNQX, 40 APV, 1 strychnine and 20 bicuculline to minimize KCC2-independent Cl^- transport. MQAE fluorescence was measured using a Zeiss LSM 510 laser scanning microscope coupled to a femtosecond pulsed Ti-Sapphire laser (Chameleon Ultra, Coherent, CA, USA) tuned at 750nm. Fluorescence was acquired through a 40X water-immersion objective (Zeiss, 0.8 NA) and, a band-pass filter (390–465 nm). Recorded cells were identified as L_I cells merging transmitted light and MQAE fluorescence. MQAE images were acquired every 5 s. After a control period of 75 s, perfusion solution was switched to

ACSF containing 15 mM KCl (osmolarity adjusted using mannitol) to reverse Cl^- transport[24]. The average fluorescence from each cell body and was expressed as $\%\Delta F/F_0$. Fluorescence lifetimes were measured in control and after Cl^- equilibrium was achieved in 15 mM extracellular KCl to obtain quantitative estimates of $[Cl^-]_i$ independent of $[MQAE]_i$[19]. To ensure that measurements of rates of intracellular Cl^- loading were performed for comparable $[Cl^-]_i$, exposure to 15 mM KCl was initiated after sufficient incubation time, so that the steady-state $[Cl^-]_i$ was comparable in control and morphine conditions. MQAE lifetime was recorded with a Becker & Hickl SPC-830 module through the nondescanned port of the Zeiss LSM 510 using a band-pass filter (469/35 nm, Semrock, NY, USA) coupled to a laser block (short-pass 750 nm; Semrock). Photon emission was detected using a PMC-100-1 photosensor (Hamamatsu, Japan). Lifetime in each cell was averaged over the cell body area and extracted using SPCImage software (Becker & Hickl, Germany). Instrument response function of the detection path was acquired using a 80nm gold nanoparticle suspension to generate second-harmonic signal. Absolute $[Cl^-]_i$ was calculated from a calibration of the Cl^- dependence of MQAE lifetime as described[19].

Microglia primary culture preparation

Primary culture was prepared as described[27]. Briefly, mixed glial culture was isolated using postnatal (P1–P3) rat cortex and maintained for 10–14 days in DMEM medium containing 10% fetal bovine serum (Invitrogen, ON, Canada). Microglia separated by gentle shaking were plated, and treated with morphine (100 nM), morphine/naloxone (1 μM), morphine/(+)naloxone (1 μM), morphine/LPS-RS (1, 10, 100 ng/ml; Invivogen), morphine/TNP-ATP (10 μM; Sigma), morphine/PPADS (pyridoxal-phosphate-6-azophenyl-2′,4′-disulfonate, 10 μM; Sigma), morphine/TrkB-Fc (5 μg/ml, R&D Systems), or morphine/IgG-Fc (5 μg/ml, R&D Systems) once daily for 5 days. Control cultures were treated with either PBS or the above drugs in the absence of morphine once daily for 5 days.

Microglia calcium imaging

Cells were incubated at RT for 30 min with Fura-2 AM (2.5 μM; Molecular Probes, OR, USA) in ACSF containing (in mM) NaCl 140, KCl 5.4, $CaCl_2$ 1.3, HEPES 10, glucose 33, pH 7.35, osmolarity 315–320 mOsm. ATP (50 μM; Sigma) was bath-applied. Excitation light was generated from a 75 W xenon arc lamp and passed alternatingly through 340 or 380 nm bandpass filters[56] (Omega Optical, VT, USA).

Microglia whole cell recording

ACSF was as above, except for (in mM) $MgCl_2$ 1 and $CaCl_2$ 2. Pipettes contained (in mM): CsCl 140, $MgCl_2$ 1, BAPTA 10, HEPES 10, pH 7.2 ATP (50 μM) was applied for 2 s using a fast-step perfusion system (SF-77B, Warner Instruments, CT, USA) and recorded using an Axopatch 1-D amplifier (Molecular Devices). The electrical signals were digitized with a DigiData 1200 (Molecular Devices) and filtered at 2 kHz.

Intrathecal injections of microglia

These experiments were performed as described[57]. Briefly, prior to intrathecal injection, microglia cultures were washed out in PBS, removed from the dish surface using a cell

scraper and collected in 100 μl of PBS. Cell density was measured using a cell counter and the volume of PBS adjusted to give a final density of 1000 cells/10 μl. This preparation was injected via lumbar puncture. Paw withdrawal threshold was tested prior to injection, after 1, 3, and 5 h. In a previous set of experiments with intrathecal catheter implants, microglia was shown to produced a significant effect on withdrawal reflex only when administered dorsally, confirming a selective action at the SDH level (Supplementary Fig. 3).

Western blotting

Cultured microglia were harvested and collected in 100 μl of PBS containing a phosphatase inhibitor cocktail (2%, Sigma) and a broad spectrum protease inhibitor (2%, Sigma). After centrifugation, the pellet was resuspended in 3% sodium dodecyl sulfate (SDS) containing 15% glycerol and 75 mM Tris-base. Total protein was measured using a BCA protein assay reagent kit (Pierce, IL, USA). Samples were heated at 95°C for 10 min in 2X sample buffer (Pierce), electrophoresed on a precast SDS polyacrylamide gradient gel (4%–12% Tris-HCl; Bio-Rad) and transferred onto a nitrocellulose membrane. After blocking, membranes were incubated with rabbit anti-P2X4R (1:1000; Alomone) or mouse anti-actin (1:5000; Sigma), followed by incubation with HRP-conjugated secondary antibody, ECL detection (Amersham) and densitometric quantification (Image J software, NIH). Rat spinal cords were rapidly dissected and frozen in liquid nitrogen. Spinal cord homogenates were separated on a precast SDS polyacrylamide gradient gel (4–12% Tris-HCl; Bio-Rad) or 4–12% Tris glycine gel (Invitrogen) and transferred onto nitrocellulose membrane. P2X4R detection was performed as described above. For KCC2 detection, gel loading was done in a Laemmli sample buffer (Biorad) containing 0.5% Lithium dodecyl sulfate (LDS) to solubilize KCC2. Membranes were incubated in PBS/milk (pH 7.4) and incubated overnight with the polyclonal rabbit anti-KCC2 (1:1000; Millipore, MA, USA, #-07-432)[23] at 4°C. Membranes were washed and incubated for 2 h at RT in rabbit specific secondary antibody then quantified by direct detection of secondary antibody fluorescence at 700 and 800nm (Odyssey Licor; USA). The relative amount of monomeric or oligomeric KCC2 was calculated as described[23]. Full-length blots are shown in Supplementary Fig. 4.

Histological procedures

Rats or mice were anesthetized and perfused transcardially with 4% paraformaldehyde in 0.1 M PB (pH 7.4). Spinal cord sections were obtained as described[58]. Sections were incubated overnight at 4°C in rabbit anti-KCC2 1:1000, guinea pig anti-μ-receptor antibody 1:5000 (Neuromics, MN, USA), mouse OX-42 anti-CD11b 1:500 (Millipore) or 1:1000 (Serotec, NC, USA). After washing, sections were incubated at RT in a solution containing appropriate fluorochrome-conjugated secondary antibodies. Images were obtained with an Olympus FV300-IX71 confocal microscope (Olympus America Inc., NY, USA) for KCC2 staining or with a Leica TCS SP2 confocal microscope (Leica) for CD11b immunocytochemistry (ICC). Images of CD11b ICC from intrathecal saporin/saporin-mac1 experiments were acquired with a fluorescence microscope (Olympus). Laminar boundaries were identified as described[58]. Quantification was performed using ImageJ for CD11b ICC and using locally designed software for KCC2 (The MathWorks Inc., MA, USA). β-galactosidase activity in *P2rx4*$^{-/-}$ mouse spinal cords was revealed by incubation with a solution of X-Gal (1 mg/ml), 5 mM K^+-ferrycyanide, 2 mM $MgCl_2$, 0.2% Triton X-100 in

PBS o.n. at 37°C. X-gal staining was quantified using ImageJ. No staining was detected in wild type mice.

Enzyme-Linked Immunosorbent Assay (ELISA)

Recovery of BDNF released from microglia was achieved using a Microcon YM-10 centrifugal filter device (Millipore). As described[22], measurement of microglial BDNF was performed using a specific ELISA kit (detection range: 7.8 pg/ml to 500 pg/ml) with BDNF standards (7.82–500 pg/ml) and 100 μl of supernatant sample run in triplicate (Chemicon, CA, USA). Samples were washed and incubated with biotinylated mouse anti-BDNF monoclonal antibody, incubated with streptavidin-HRP conjugate, treated with 3,3′,5,5′-tetramethylbenzidine substrate and read by a spectrophotometer plate reader (Molecular Devices) at 450 nm. Samples were considered BDNF positive if their signal was higher than the background signal and within the range of the standard curve. Data were normalized to the control.

Statistics

All data are given as the mean ± s.e.m. As data distribution poorly fit with Gaussian distribution, non-parametric tests were used (unless otherwise stated). Differences between groups were tested by Mann-Whitney test or by Kruskal-Wallis test with *post-hoc* Dunn test. Repeated measures were analyzed by Friedmann test with *post-hoc* Dunnet test or Wilcoxon test. Fisher's exact test was used for contingency tables. Bi-exponential fittings were compared by F-test. Sample sizes are in line with those reported in similar studies. Differences were considered significant for $P < 0.05$.

Supplementary Material

Refer to Web version on PubMed Central for supplementary material.

Acknowledgments

This work was supported by Canadian Institutes for Health Research (CIHR) grants to YDK, MWS, CC and JMB, by the Krembil Foundation to YDK and MWS, and the Ontario Research Fund Research Excellence Program to MWS. FF is the recipient of a Regione Piemonte/University of Turin fellowship; TT and LL were supported by CIHR fellowships; YDK a *Chercheur National* of the Fonds de la recherche en santé du Québec (FRSQ); MWS is a Howard Hughes International Research Scholar and holder of a Tier 1 Canada Research Chair; CC and JMB are holders of Tier 2 Canada Research Chairs. We thank Karine Bachand for technical assistance with behaviour, Dr. François Rassendren (INSERM, France) for *P2rx4*$^{-/-}$mice, Dr. Christopher J. Evans (NIDA, USA) for (+)naloxone and Dr. Jason Vlahakis for (+)naloxone polarimetric analysis.

References

1. Bekhit MH. Opioid-induced hyperalgesia and tolerance. Am J Ther. 2010; 17:498–510. [PubMed: 20844348]
2. Lee M, Silverman SM, Hansen H, Patel VB, Manchikanti L. A comprehensive review of opioid-induced hyperalgesia. Pain Physician. 2011; 14:145–161. [PubMed: 21412369]
3. Mao J, Sung B, Ji RR, Lim G. Chronic morphine induces downregulation of spinal glutamate transporters: implications in morphine tolerance and abnormal pain sensitivity. J Neurosci. 2002; 22:8312–8323. [PubMed: 12223586]

4. Vanderah TW, et al. Tonic descending facilitation from the rostral ventromedial medulla mediates opioid-induced abnormal pain and antinociceptive tolerance. J Neurosci. 2001; 21:279–286. [PubMed: 11150345]
5. Heinke B, Gingl E, Sandkuhler J. Multiple targets of mu-opioid receptor-mediated presynaptic inhibition at primary afferent Adelta- and C-fibers. J Neurosci. 2011; 31:1313–1322. [PubMed: 21273416]
6. Zeng J, Thomson LM, Aicher SA, Terman GW. Primary afferent NMDA receptors increase dorsal horn excitation and mediate opiate tolerance in neonatal rats. J Neurosci. 2006; 26:12033–12042. [PubMed: 17108177]
7. Woolf CJ, Salter MW. Neuronal plasticity: increasing the gain in pain. Science. 2000; 288:1765–1769. [PubMed: 10846153]
8. Craig AD. Pain mechanisms: labeled lines versus convergence in central processing. Annu Rev Neurosci. 2003; 26:1–30. [PubMed: 12651967]
9. Drdla R, Gassner M, Gingl E, Sandkuhler J. Induction of synaptic long-term potentiation after opioid withdrawal. Science. 2009; 325:207–210. [PubMed: 19590003]
10. Sandkuhler J. Models and mechanisms of hyperalgesia and allodynia. Physiol Rev. 2009; 89:707–758. [PubMed: 19342617]
11. Zeilhofer HU, Benke D, Yevenes GE. Chronic pain States: pharmacological strategies to restore diminished inhibitory spinal pain control. Annu Rev Pharmacol Toxicol. 2012; 52:111–133. [PubMed: 21854227]
12. Coull JA, et al. Trans-synaptic shift in anion gradient in spinal lamina I neurons as a mechanism of neuropathic pain. Nature. 2003; 424:938–942. [PubMed: 12931188]
13. Keller AF, Beggs S, Salter MW, De Koninck Y. Transformation of the output of spinal lamina I neurons after nerve injury and microglia stimulation underlying neuropathic pain. Mol Pain. 2007; 3:27. [PubMed: 17900333]
14. Cordero-Erausquin M, Coull JA, Boudreau D, Rolland M, De Koninck Y. Differential maturation of GABA action and anion reversal potential in spinal lamina I neurons; impact of chloride extrusion capacity. J Neurosci. 2005; 25:9613–9623. [PubMed: 16237166]
15. Sjogren P, Jonsson T, Jensen NH, Drenck NE, Jensen TS. Hyperalgesia and myoclonus in terminal cancer patients treated with continuous intravenous morphine. Pain. 1993; 55:93–97. [PubMed: 8278214]
16. Hewitt SA, Wamsteeker JI, Kurz EU, Bains JS. Altered chloride homeostasis removes synaptic inhibitory constraint of the stress axis. Nat Neurosci. 2009; 12:438–443. [PubMed: 19252497]
17. Kemp T, Spike RC, Watt C, Todd AJ. The mu-opioid receptor (MOR1) is mainly restricted to neurons that do not contain GABA or glycine in the superficial dorsal horn of the rat spinal cord. Neuroscience. 1996; 75:1231–1238. [PubMed: 8938756]
18. Smirnov S, Paalasmaa P, Uusisaari M, Voipio J, Kaila K. Pharmacological isolation of the synaptic and nonsynaptic components of the GABA-mediated biphasic response in rat CA1 hippocampal pyramidal cells. J Neurosci. 1999; 19:9252–9260. [PubMed: 10531429]
19. Doyon N, et al. Efficacy of synaptic inhibition depends on multiple, dynamically interacting mechanisms implicated in chloride homeostasis. PLoS Comput Biol. 2011; 7:e1002149. [PubMed: 21931544]
20. Staley KJ, Soldo BL, Proctor WR. Ionic mechanisms of neuronal excitation by inhibitory GABAA receptors. Science. 1995; 269:977–981. [PubMed: 7638623]
21. Prescott SA, Sejnowski TJ, De Koninck Y. Reduction of anion reversal potential subverts the inhibitory control of firing rate in spinal lamina I neurons: towards a biophysical basis for neuropathic pain. Mol Pain. 2006; 2:32. [PubMed: 17040565]
22. Coull JA, et al. BDNF from microglia causes the shift in neuronal anion gradient underlying neuropathic pain. Nature. 2005; 438:1017–1021. [PubMed: 16355225]
23. Blaesse P, et al. Oligomerization of KCC2 correlates with development of inhibitory neurotransmission. J Neurosci. 2006; 26:10407–10419. [PubMed: 17035525]
24. Chorin E, et al. Upregulation of KCC2 activity by zinc-mediated neurotransmission via the mZnR/GPR39 receptor. J Neurosci. 2011; 31:12916–12926. [PubMed: 21900570]

25. Beggs S, Salter MW. Microglia-neuronal signalling in neuropathic pain hypersensitivity 2.0. Curr Opin Neurobiol. 2010; 20:474–480. [PubMed: 20817512]
26. Zhao P, Waxman SG, Hains BC. Extracellular signal-regulated kinase-regulated microglia-neuron signaling by prostaglandin E2 contributes to pain after spinal cord injury. J Neurosci. 2007; 27:2357–2368. [PubMed: 17329433]
27. Tsuda M, et al. P2X4 receptors induced in spinal microglia gate tactile allodynia after nerve injury. Nature. 2003; 424:778–783. [PubMed: 12917686]
28. Tsuda M, Tozaki-Saitoh H, Inoue K. Pain and purinergic signaling. Brain Res Rev. 2010; 63:222–232. [PubMed: 19931560]
29. Trang T, Beggs S, Wan X, Salter MW. P2X4-receptor-mediated synthesis and release of brain-derived neurotrophic factor in microglia is dependent on calcium and p38-mitogen-activated protein kinase activation. J Neurosci. 2009; 29:3518–3528. [PubMed: 19295157]
30. Ulmann L, et al. Up-regulation of P2X4 receptors in spinal microglia after peripheral nerve injury mediates BDNF release and neuropathic pain. J Neurosci. 2008; 28:11263–11268. [PubMed: 18971468]
31. De Koninck Y. Altered chloride homeostasis in neurological disorders: a new target. Curr Opin Pharmacol. 2007; 7:93–99. [PubMed: 17182282]
32. Mannion RJ, et al. Neurotrophins: peripherally and centrally acting modulators of tactile stimulus-induced inflammatory pain hypersensitivity. Proc Natl Acad Sci U S A. 1999; 96:9385–9390. [PubMed: 10430952]
33. Boillee S, et al. Onset and progression in inherited ALS determined by motor neurons and microglia. Science. 2006; 312:1389–1392. [PubMed: 16741123]
34. Rios M, et al. Conditional deletion of brain-derived neurotrophic factor in the postnatal brain leads to obesity and hyperactivity. Mol Endocrinol. 2001; 15:1748–1757. [PubMed: 11579207]
35. Matthes HW, et al. Loss of morphine-induced analgesia, reward effect and withdrawal symptoms in mice lacking the mu-opioid-receptor gene. Nature. 1996; 383:819–823. [PubMed: 8893006]
36. Horvath RJ, Romero-Sandoval EA, De Leo JA. Inhibition of microglial P2X4 receptors attenuates morphine tolerance, Iba1, GFAP and mu opioid receptor protein expression while enhancing perivascular microglial ED2. Pain. 2010; 150:401–413. [PubMed: 20573450]
37. Hutchinson MR, et al. Exploring the neuroimmunopharmacology of opioids: an integrative review of mechanisms of central immune signaling and their implications for opioid analgesia. Pharmacol Rev. 2011; 63:772–810. [PubMed: 21752874]
38. Xu J, Xu M, Rossi GC, Pasternak GW, Pan YX. Identification and characterization of seven new exon 11-associated splice variants of the rat mu opioid receptor gene, OPRM1. Mol Pain. 2011; 7:9. [PubMed: 21255438]
39. Wang X, et al. Morphine activates neuroinflammation in a manner parallel to endotoxin. Proc Natl Acad Sci U S A. 2012; 109:6325–6330. [PubMed: 22474354]
40. Bohn LM, Gainetdinov RR, Lin FT, Lefkowitz RJ, Caron MG. Mu-opioid receptor desensitization by beta-arrestin-2 determines morphine tolerance but not dependence. Nature. 2000; 408:720–723. [PubMed: 11130073]
41. Mao J. Opioid-induced abnormal pain sensitivity: implications in clinical opioid therapy. Pain. 2002; 100:213–217. [PubMed: 12467992]
42. Wang Y, et al. Blockade of PDGFR-beta activation eliminates morphine analgesic tolerance. Nat Med. 2012; 18:385–387. [PubMed: 22344297]
43. Knabl J, et al. Reversal of pathological pain through specific spinal GABAA receptor subtypes. Nature. 2008; 451:330–334. [PubMed: 18202657]
44. Asiedu M, Ossipov MH, Kaila K, Price TJ. Acetazolamide and midazolam act synergistically to inhibit neuropathic pain. Pain. 2010; 148:302–308. [PubMed: 20007010]
45. Horvath RJ, DeLeo JA. Morphine enhances microglial migration through modulation of P2X4 receptor signaling. J Neurosci. 2009; 29:998–1005. [PubMed: 19176808]
46. Takayama N, Ueda H. Morphine-induced chemotaxis and brain-derived neurotrophic factor expression in microglia. J Neurosci. 2005; 25:430–435. [PubMed: 15647486]

47. Merighi A, et al. BDNF as a pain modulator. Prog Neurobiol. 2008; 85:297–317. [PubMed: 18514997]
48. Zhao J, et al. Nociceptor-derived brain-derived neurotrophic factor regulates acute and inflammatory but not neuropathic pain. Mol Cell Neurosci. 2006; 31:539–548. [PubMed: 16413788]
49. Boulenguez P, et al. Down-regulation of the potassium-chloride cotransporter KCC2 contributes to spasticity after spinal cord injury. Nat Med. 2010; 16:302–307. [PubMed: 20190766]
50. Vargas-Perez H, et al. Ventral tegmental area BDNF induces an opiate-dependent-like reward state in naive rats. Science. 2009; 324:1732–1734. [PubMed: 19478142]
51. Sim JA, et al. Altered hippocampal synaptic potentiation in P2X4 knock-out mice. J Neurosci. 2006; 26:9006–9009. [PubMed: 16943557]
52. Poltorak A, et al. Defective LPS signaling in C3H/HeJ and C57BL/10ScCr mice: mutations in Tlr4 gene. Science. 1998; 282:2085–2088. [PubMed: 9851930]
53. Wang Y, et al. Age-dependent morphine tolerance development in the rat. Anesth Analg. 2005; 100:1733–1739. [PubMed: 15920206]
54. Trang T, Ma W, Chabot JG, Quirion R, Jhamandas K. Spinal modulation of calcitonin gene-related peptide by endocannabinoids in the development of opioid physical dependence. Pain. 2006; 126:256–271. [PubMed: 16935424]
55. Yaksh TL, Jessell TM, Gamse R, Mudge AW, Leeman SE. Intrathecal morphine inhibits substance P release from mammalian spinal cord in vivo. Nature. 1980; 286:155–157. [PubMed: 6157098]
56. Salter MW, Hicks JL. ATP causes release of intracellular Ca2+ via the phospholipase C beta/IP3 pathway in astrocytes from the dorsal spinal cord. J Neurosci. 1995; 15:2961–2971. [PubMed: 7722640]
57. De la Calle JL, Paino CL. A procedure for direct lumbar puncture in rats. Brain Res Bull. 2002; 59:245–250. [PubMed: 12431755]
58. Lorenzo LE, Ramien M, St Louis M, De Koninck Y, Ribeiro-da-Silva A. Postnatal changes in the Rexed lamination and markers of nociceptive afferents in the superficial dorsal horn of the rat. J Comp Neurol. 2008; 508:592–604. [PubMed: 18383051]

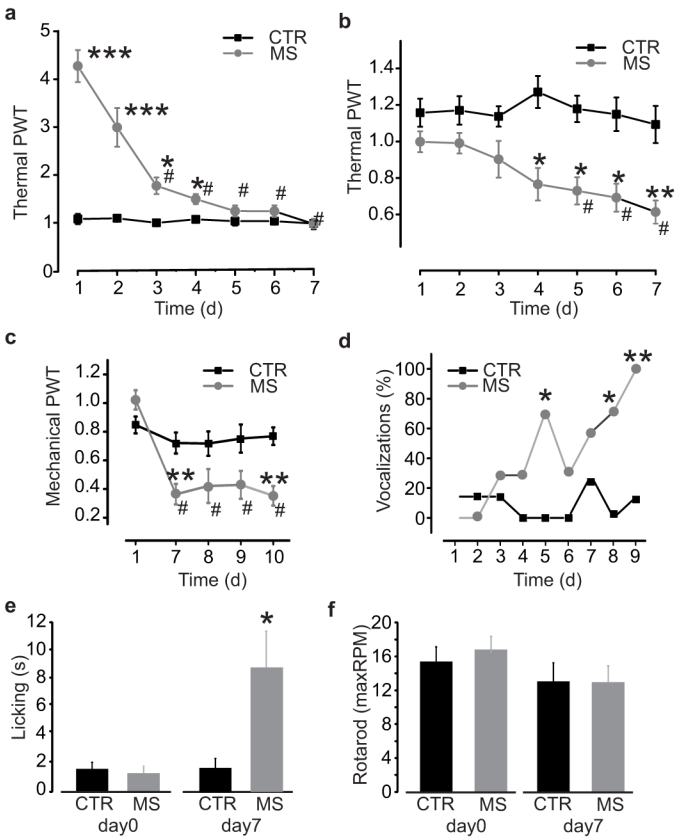

Figure 1. Repeated morphine administration causes hyperalgesia and tolerance

a–c. Time course of morphine tolerance and pain hypersensitivity assessed by Hargreaves plantar test and von Frey filament in rats: **a.** Thermal pain threshold 1h after morphine (days 3–7 *vs* day 1, χ^2: 61.5; $^{\#}P < 0.001$) or saline injection (morphine *vs* saline at days 1–4, $^{*}P < 0.05$; $^{***}P < 0.001$); **b**. Thermal pain threshold before morphine (days 5–7 *vs* day 1, χ^2: 20.7; $^{\#}P < 0.001$) and saline injection (morphine *vs* saline at days 4–7, $^{*}P < 0.05$; $^{**}P < 0.01$); **c**. Mechanical pain threshold before morphine or saline injection. At day 7, threshold of morphine treated rats ($n = 7$) is significantly reduced as compared to day 1 (χ^2: 13.58, $^{\#}P < 0.01$) and to the saline group ($n = 6$; $^{**}P < 0.01$). **d–e**. Progressive increase in nociceptive behaviours in morphine-treated rats as compared to saline-treated controls: **d**. Percentage of vocalizing rats during subcutaneous injections (day 5–9 *vs* day 1, $^{*}P < 0.05$; $^{**}P < 0.01$); **e**. Licking time after thermal stimulation (day 0, $P > 0.05$; day 7, U: 7, $^{*}P < 0.05$). **f**. Maximal running speed at day 0 and day 7 of saline or morphine injections assessed by rotarod before the morning injection (U: 21, $P > 0.05$). All threshold values are normalized to the baseline. Abb.: PWT = paw withdrawal threshold; CTR = saline control; MS = morphine sulphate; RPM = revolutions per minute; error bars = s.e.m.

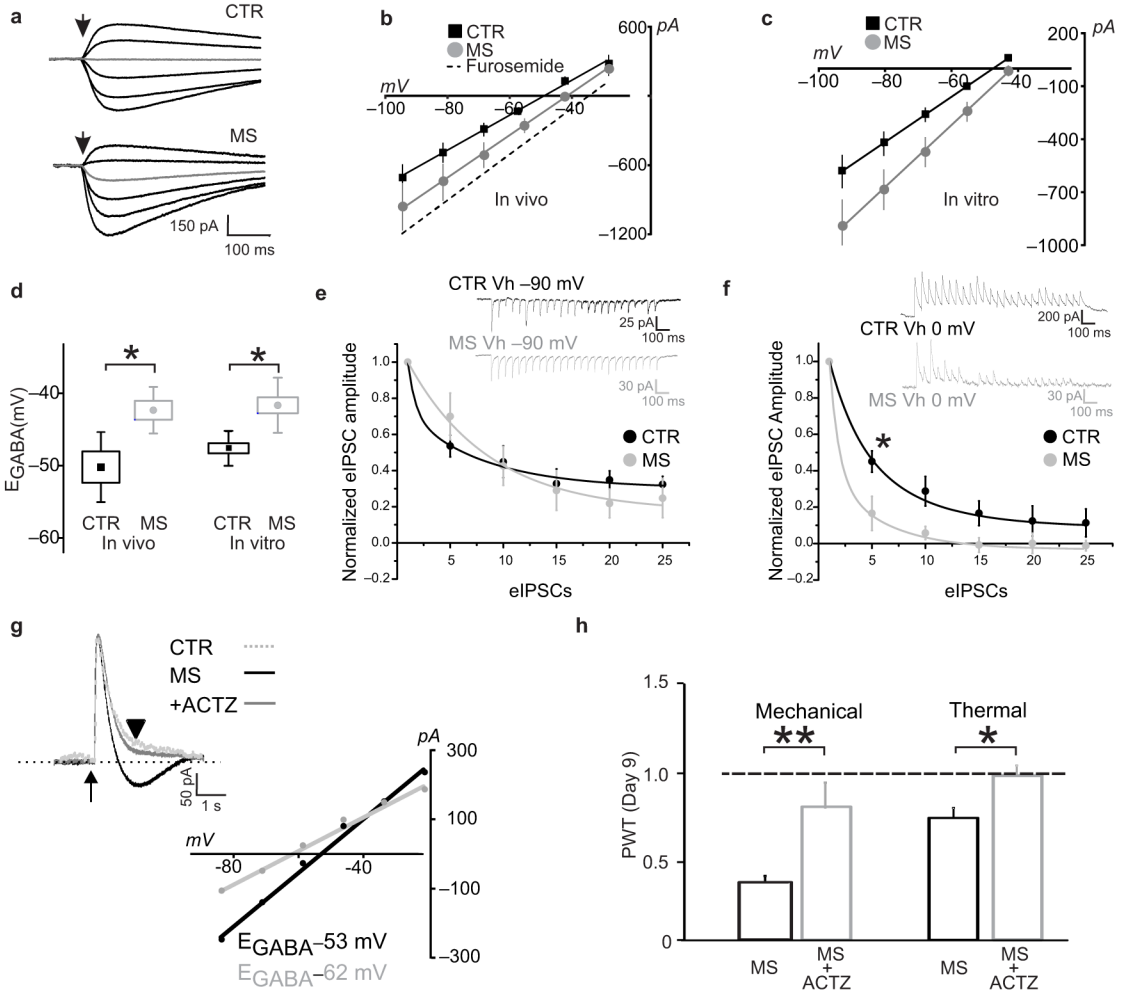

Figure 2. Morphine disrupts Cl^- homeostasis in L_I neurons

a–b. Decrease in Cl^- extrusion capacity in L_I neurons after *in vivo* morphine treatments in rats: **a.** Responses to GABA 30 ms puffs following saline- or morphine-treatments in presence of a Cl^- load (29 mM). In *grey*, the response obtained at −55.5 mV. **b**. I-V relationships for $GABA_A$ currents obtained from morphine-treated rats ($n = 6$ cells) is right-shifted as compared to controls ($n = 5$ cells); *dashed line* indicates the I–V relationship when Cl^- extrusion capacity is blocked by the KCC2 antagonist furosemide. **c**. Effect of in vitro morphine (1 μM, > 3 h; $n = 7$ cells) on I–V relationships for $GABA_A$ currents *vs* saline control ($n = 6$ cells). **d**. Pooled E_{GABA} of neurons shown in **b** (U: 2) and **c** (U: 6, $^*P < 0.05$). **e–f**. Cl^- accumulation under repetitive inhibitory input. **e**. Representative traces (average of 10 repetitions) from a control- *black*- and an in vitro morphine-treated L_I neuron- *grey*-clamped at −90 mV (*upper panel*); in the graph (*lower panel*), the rate of eIPSC amplitude depression during repetitive stimulation (20 Hz). Amplitude values are normalized to the first eISPC. No differences were observed (CTR: $n = 6$; MS: $n = 4$ cells; F: 0.8, $P > 0.05$). **f**. Experiment in **e** repeated at 0 mV. Note the larger and faster eIPSC depression in morphine-treated neurons. Differences between morphine and controls are significant (CTR: $n = 6$; MS: $n = 4$ cells; F: 21.98, $^*P < 0.05$). **g**. Gramicidin-perforated patch clamp recording of

GABA responses obtained at −60 mV in control –*red dotted line*- and from a morphine treated L_I neuron before (*in black*) and after ACTZ (50 μM; *in grey*; traces are scaled to the peak amplitude; *arrow* indicates the GABA puff). Note the biphasic response in the morphine neuron and the monophasic response following ACTZ. Below, I-V curves measured 1 s after the pulse (*black arrowhead*). Note the increased E_{GABA} difference before and after acetazolamide. **h**. Effect of intrathecal ACTZ (22.5 μg, from day 7 to 9) on morphine-induced mechanical (saline, $n = 5$; ACTZ, $n = 5$; U: 0, $^{**}P < 0.01$) and thermal (saline, $n = 11$; ACTZ, $n = 9$; U: 15.5, $^{*}P < 0.05$) pain hypersensitivity in rats. All threshold values are normalized to the baseline. *dashed line* is the baseline threshold. Abb.: PWT = paw withdrawal threshold; CTR = control; MS = morphine sulphate; ACTZ = acetazolamide; error bars = s.e.m.

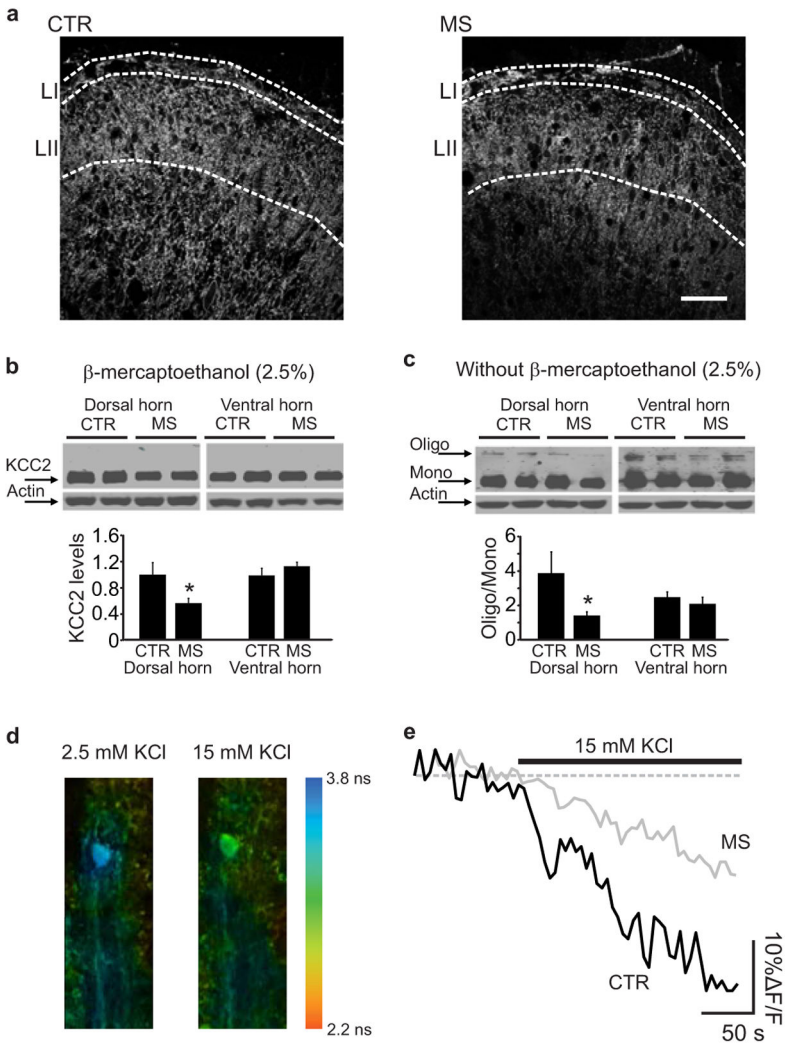

Figure 3. Morphine effects on activity and expression of KCC2

a. KCC2 immunostaining in rat L_I and L_{II} following 7 days of saline or morphine injections (scale bar, 50 μm). **b.** Western blot showing the total KCC2 expression in the dorsal and ventral horn from saline- and morphine-treated rats. Histograms show quantification of KCC2 expression normalized to the actin level in the dorsal (one-tail t-test, t: 2.1, $*P < 0.05$) and ventral horn (one-tail t-test, t: −1.1, $P > 0.05$). **c**. Western blot performed without β-mercaptoethanol to preserve KCC2 oligomerization. The histograms show quantification of KCC2 oligmer/monomer ratio in the dorsal (one-tail t-test, t: 2.1, $*P < 0.05$) and the ventral horn (one-tail t-test, t: 0.6, $P > 0.05$). **d–e.** Chloride imaging from rat spinal cord slices loaded with the Cl^- -sensitive dye MQAE. **d**. Pseudocolor images show lifetime maps from a control L_I neuron in presence of 2.5 or 15 mM KCl. Lifetimes from L_I neurons in control conditions (3.44 ± 0.34 ns, n =11 cells) were significantly shortened (reflecting quenching of MQAE fluorescence) 15 minutes after exposure to high extracellular KCl to reverse KCC2 transport (3.02 ± 0.24 ns, n =11; $P < 0.001$). **e**. Representative traces of fluorescence intensity in control (*black*) and morphine-treated neuron (*grey*) showing the rate of intracellular Cl^- accumulation ($\%\Delta F/F_0$) in the presence of 15 mM KCl. Steady-state

lifetime measurements just prior to 15 mM KCl solutions were not different (3.37 ± 0.06 and 3.23 ± 0.06 ns in control *vs* morphine, respectively; corresponding to 7.0 ± 0.7 and 8.6 ± 0.8 mM of Cl^- in control *vs* morphine, respectively; U: 38, $P > 0.05$). Abb.: CTR = saline control; MS = morphine sulphate; error bars = s.e.m.

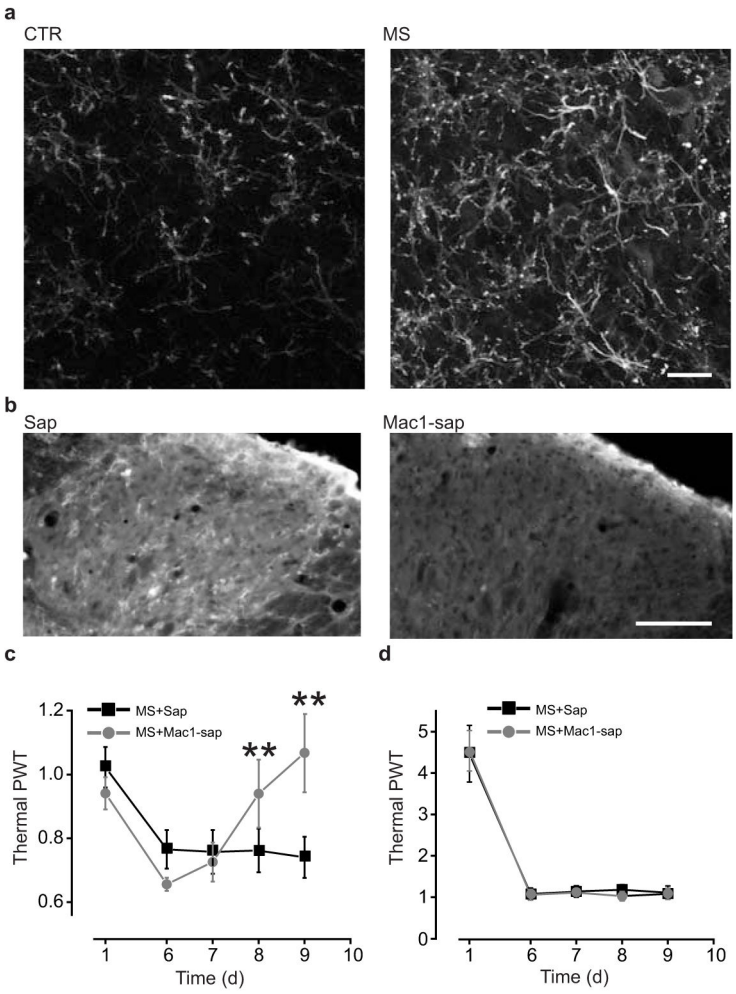

Figure 4. Morphine-induced hyperalgesia depends on microglia activation

a. CD11b expression in rat SDH following 5 days of saline or morphine treatment (scale bar, 30 μm) and fluorescence intensity quantification (CTR: 0.84 ± 0.06 i.u., $n = 28$ sections; MS: 2.78 ± 0.22 i.u., $n = 34$ sections; U: 8, $P < 0.001$). **b–d.** Effects of intrathecal injection of anti-mac1saporin-conjugated antibody (*vs* saporin alone) on SDH CD11b expression, morphine-induced hyperalgesia and tolerance (intrathecal injections were performed from day 7 to 9 of morphine treatment): **b**. CD11b expression in SDH after microglia depletion with anti-mac1 antibody (scale bar 50 μm) (sap: 10.12 ± 1.32 i.u., $n = 17$ sections; mac-1-sap: 7.84 ± 2.23 i.u., $n = 16$ sections; U: 55, $^{**}P < 0.01$); **c.** Thermal pain threshold before morphine injection (mac1-saporin *vs* saporin alone at day 9, U: 1; $^{**}P < 0.01$); **d.** Thermal pain threshold 1h after morphine injection (day 9, U: 12, $P > 0.05$). All threshold values in the figure are normalized to the baseline. Abb.: PWT = paw withdrawal threshold; CTR = control; MS = morphine sulphate; sap = saporin; mac1-sap = saporin-conjugated anti-mac1 antibody; error bars = s.e.m.

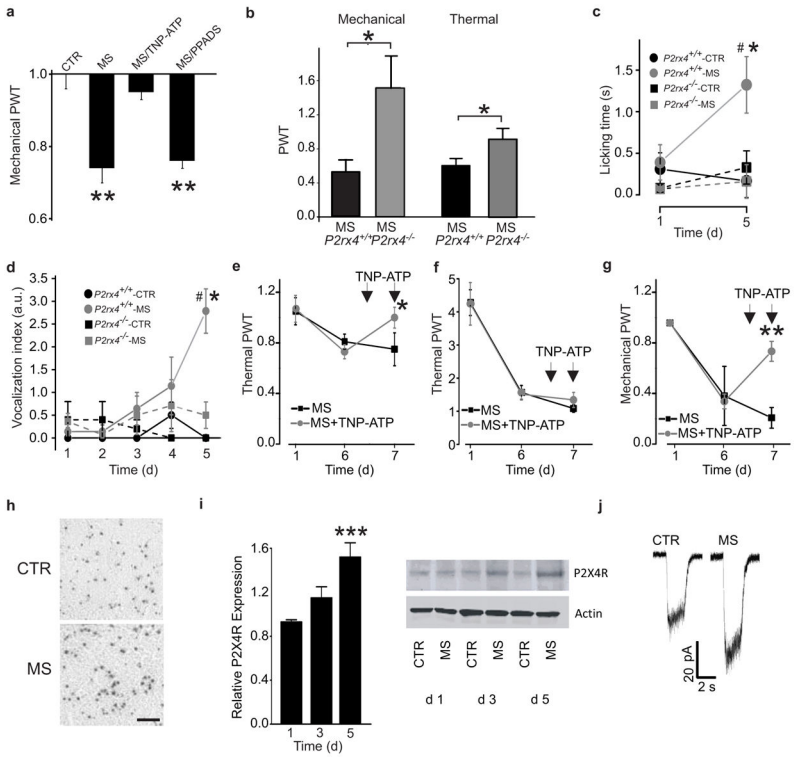

Figure 5. P2X4Rs in microglia are required for morphine-induced hyperalgesia

a. Rat mechanical pain threshold 5 h after intrathecal injections of cultured microglia treated with morphine (100 nM, $n = 7$; H: 19.98, $^{**}P < 0.01$), morphine+TNP-ATP ($n = 5$, $^{*}P > 0.05$), morphine+PPADS ($n = 8$; $^{**}P < 0.01$), *vs* CTR ($n = 7$). **b–d**. Lack of hyperalgesia in *P2rx4*$^{-/-}$mice: **b.** Thermal ($n = 5$ mice per group) and mechanical ($n = 7$ mice per group) pain threshold after 5 days of subcutaneous morphine injections in *P2rx4*$^{+/+}$ mice vs *P2rx4*$^{-/-}$ mice (U: 5 for mechanical and U: 2 for thermal test, $^{*}P < 0.05$). **c**. Licking time following mechanical stimulation of the paw (morphine-treated *P2rx4*$^{+/+}$ *vs* morphine-treated *P2rx4*$^{-/-}$, $^{*}P < 0.05$; # significant differences compared to the baseline); **d**. Vocalizations produced by subcutaneous injections (morphine-treated *P2rx4*$^{+/+}$ *vs* other groups, $^{*}P < 0.05$; # significant differences compared to the baseline). **e–g**. Effect of intrathecal TNP-ATP (30 nmol) on MIH in rats: **e**. thermal pain threshold prior to morphine injection in vehicle ($n = 8$) vs TNP-ATP injected rats ($n = 8$; day 7, U: 13, $^{*}P < 0.05$); **f**. thermal pain threshold 1 h after morphine. **g**. Mechanical withdrawal threshold following TNP-ATP in morphine-treated rats measured prior to morphine injection (day 7, CTR, $n = 6$, TNP-ATP, $n = 7$; U: 0, $^{**}P < 0.01$). **h.** X-gal staining in *P2rx4*$^{-/-}$mice (scale bar, 30 μm). The percentage SDH staining area of control (3.6 ± 0.3%, $n = 5$ sections) and morphine-treated mice (4.8 ± 0.3%, $n = 12$ sections; U: 10, $^{*}P < 0.05$). **i–j.** Increased expression and function of P2X4R in morphine-treated (100 nM) microglia cultures: **i**. Expression of P2X4R after morphine treatment normalized to the saline controls for 1 day (d1, $n = 7$ trials), 3 days (d3, $n = 7$) and 5 days (d5, $n = 7$; H: 19.35, $^{***}P < 0.001$); **j**. ATP-mediated currents in morphine-treated microglia over 5 days (peak current normalized to the pre-ATP baseline: 1.6 ± 0.2; $n = 12$ cells; U: 91, $^{*}P < 0.05$) *vs* control (1.0 ± 0.1; $n = 28$ cells). All threshold values in the figure are normalized to the baseline. Abb.: PWT = paw withdrawal

threshold; CTR = control; MS = morphine sulphate; a.u. = arbitrary unit; X-gal = 5-bromo-4-chloro-indolyl-galactopyranoside; error bars = s.e.m.

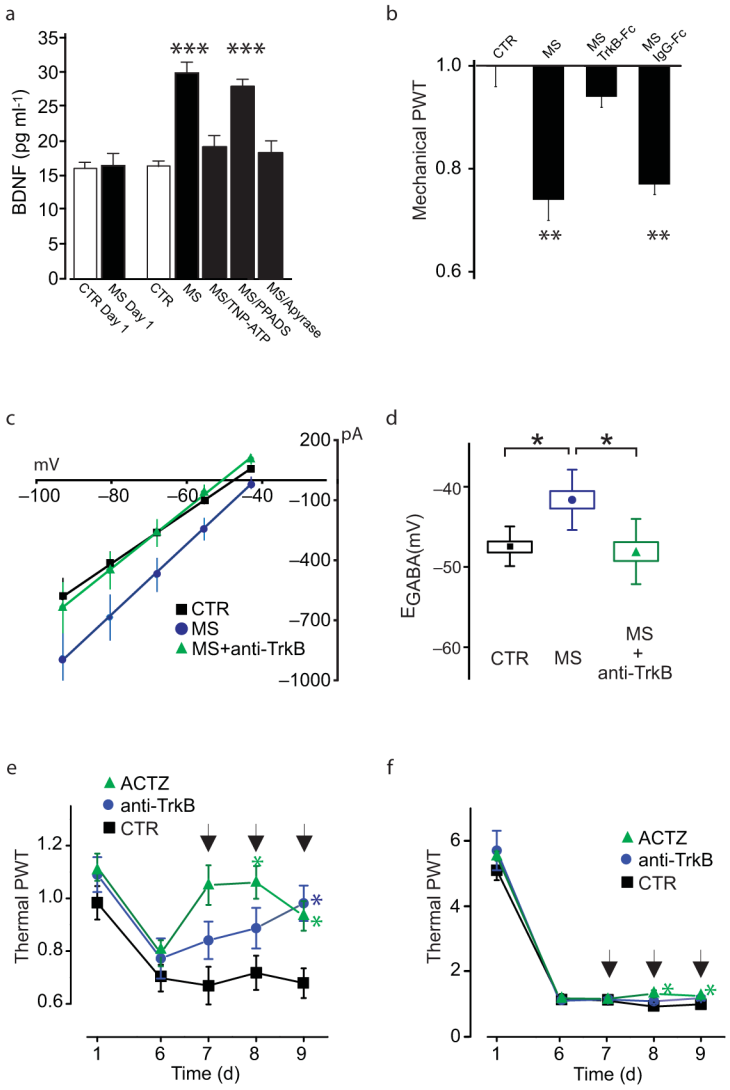

Figure 6. Altered Cl^- homeostasis in spinal neurons and morphine-induced hyperalgesia are depend on P2X4R-BDNF-TrkB signaling

a. ELISA-based measurement of BDNF release from cultured microglia treated with 100 nM morphine ($n = 14$ trials, H: 30.17, $^{***}P < 0.001$), morphine + TNP-ATP ($n = 5$, $P > 0.05$), morphine + PPADS ($n = 5$, $^{***}P < 0.001$), morphine + apyrase ($n = 5$; $P > 0.05$) *vs* saline ($n = 14$). **b**. Rat mechanical withdrawal threshold 5 h after intrathecal injection of morphine treated microglia ($n = 7$; H: 23.66, $^{**}P < 0.01$), morphine+TrkB-Fc ($n = 7$; $P > 0.05$), morphine+IgG-Fc ($n = 7$; $^{**}P < 0.01$), *vs* CTR ($n = 7$). **c–d**. Effect of anti-TrkB antibody (1 μg/ml) on morphine-induced shift of E_{GABA} in L_I neurons *in vitro*: **c**, I–V relationships for $GABA_A$ currents after incubation with morphine ($n = 12$ cells), morphine +anti-TrkB ($n = 7$) or in control ($n = 6$) and, **d**, the respective E_{GABA} values (H: 11.16, $^{*}P < 0.05$). **e–f**. Effect of intrathecal injections in rats of ACTZ and anti-TrkB on morphine-induced pain hypersensitivity and tolerance by Hargreaves plantar test: **e.** Thermal withdrawal threshold prior to morphine in ACTZ- (22.5 μg, $n = 9$), anti-TrkB- (30 μg, $n = 7$) and vehicle-injected rats ($n = 11$; day 9, $^{*}P < 0.05$; *arrows* indicate injections); **f**. Thermal

pain threshold 1h after morphine in ACTZ-, anti-TrkB- and vehicle-injected groups (ACTZ *vs* control group at days 8–9; $*P < 0.05$; *arrows* indicate injections). All threshold values are normalized to the baseline. Abb.: PWT = paw withdrawal threshold; CTR = control; MS = morphine sulphate; Anti-TrkB = anti-TrkB blocking antibody; ACTZ = acetazolamide; error bars = s.e.m.

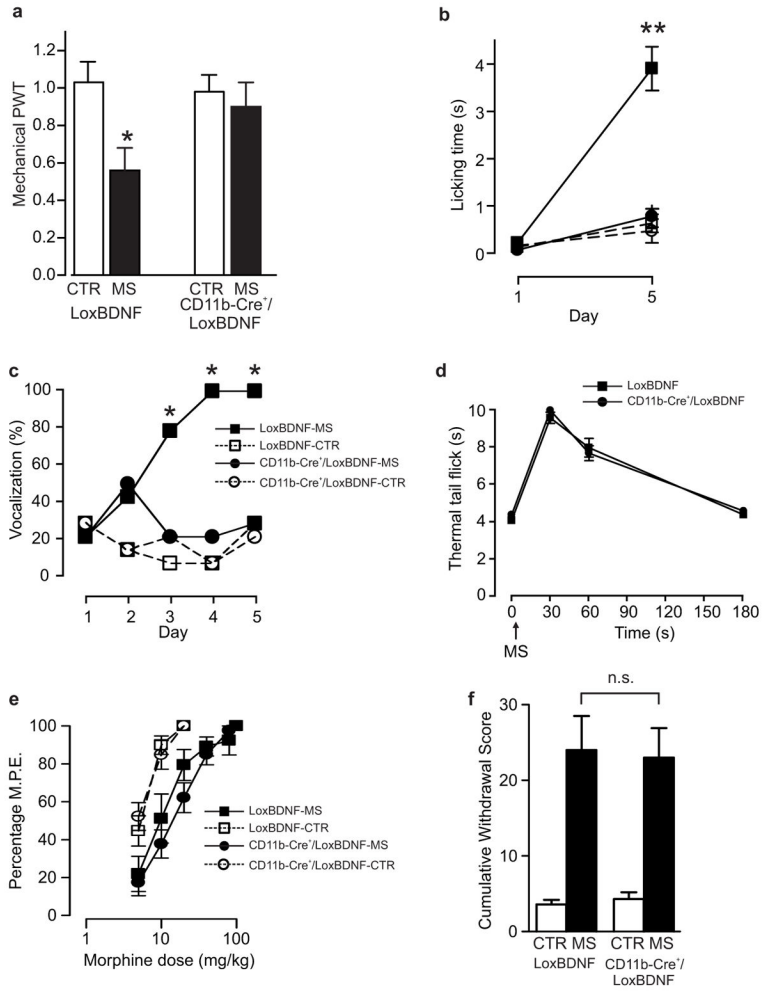

Figure 7. Genetic deletion of BDNF from microglia abrogates development of morphine-induced hyperalgesia, but not tolerance

a–c: Assessment of morphine-induced hyperalgesia in CD11b-Cre$^+$/LoxBDNF mice ($n = 7$) vs LoxBDNF mice ($n = 7$): **a**. Effect of 5 days of morphine on mechanical threshold (F: 3.499, $^*P < 0.05$); **b**. licking time following mechanical stimulation of the hindpaw (H: 16.21, $^{**}P < 0.05$); **c**. and vocalizations produced by subcutaneous injections. **d–e**: Assessment of morphine antinociception in CD11b-Cre$^+$/LoxBDNF mice ($n = 7$; $^*P < 0.05$) vs LoxBDNF mice ($n = 7$): **d.** Time course of antinociceptive response to a single dose of morphine in morphine naïve mice; **e.** Morphine dose-response curves following 5 days of morphine or saline injections in CD11b-Cre$^+$/LoxBDNF mice ($n = 7$) vs LoxBDNF mice ($n = 7$). The rightward shift in morphine-treated animals indicates the development of morphine tolerance in both CD11b-Cre$^+$/LoxBDNF and LoxBDNF mice, with no significant differences between the two genotypes. ED50 in saline injected controls were: LoxBDNF mice 3.5±0.3 mg/Kg, CD11b-Cre$^+$/LoxBDNF 3.3±0.3 mg/Kg ($P > 0.05$); ED50 in morphine-treated mice were: LoxBDNF 16.5±1.0 mg/Kg and CD11b-Cre$^+$/LoxBDNF 14.3±1.1 mg/Kg ($P > 0.05$). **f**. Naloxone-precipitated withdrawal syndrome in CD11b-Cre$^+$/LoxBDNF mice (CTR, $n = 3$; MS, $n = 6$) vs LoxBDNF mice (CTR, $n = 5$; MS, $n = 5$). Withdrawal cumulative score was significantly higher in both morphine treated groups as

compared to the saline controls, but no differences were detected between CD11b-Cre^{+}/LoxBDNF and LoxBDNF mice. All threshold values are normalized to the baseline. Abb.: PWT = paw withdrawal threshold; CTR = control; MS = morphine sulphate; error bars = s.e.m.

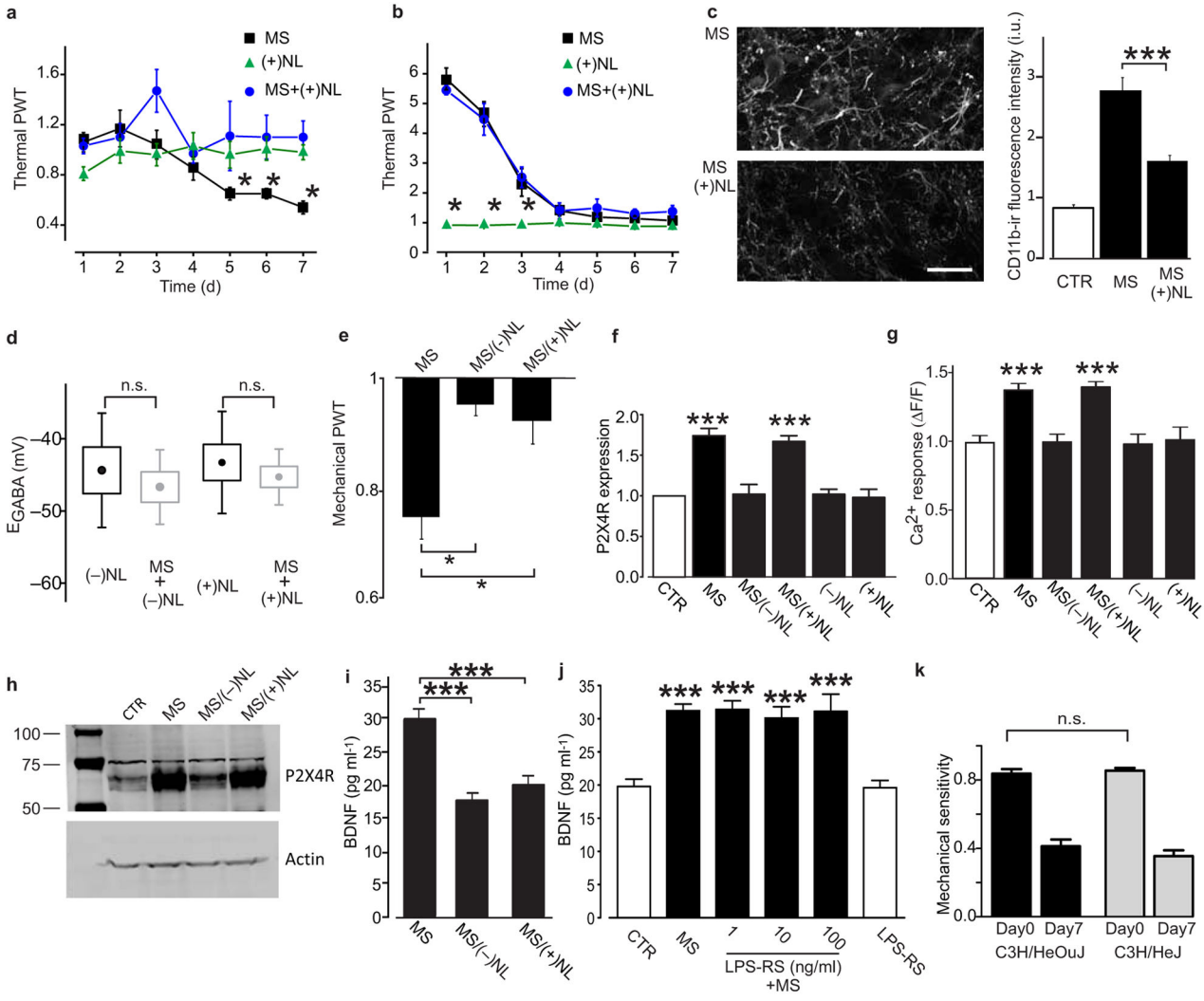

Figure 8. Activation of two separate signaling pathways is necessary for morphine-induced hyperalgesia

a–c. Effect of intrathecal injections of low doses of (+)NL (5 ng) on morphine-induced pain hypersensitivity, tolerance and microglia activation: **a.** Thermal withdrawal threshold prior to morphine or saline injections in(+)NL or vehicle treated rats ((+)NL, $n = 8$; morphine+(+)NL, $n = 7$; morphine, $n = 8$; $^{*}P < 0.05$); **b**. Thermal pain threshold 1 h after treatment. **c.** CD11b immunostaining in rat SDH following 5 days of intrathecal morphine or morphine+(+)NL (scale bar, 30 μm) and quantification (CTR: $n = 28$ sections; MS: $n = 34$ sections; morphine+(+)NL: $n = 34$ sections; $^{***}P < 0.001$). **d**. L_I E_{GABA} following 3 h *in vitro* with (−)NL alone ($n = 6$ cells) *vs* morphine+(−)NL ($n = 6$; U: 14; $P > 0.05$) and with (+)NL ($n = 6$) *vs* morphine + (+)NL ($n = 8$, U: 26; $P > 0.05$). **e.** Mechanical withdrawal threshold 5 h after intrathecal injections of microglia cultures treated with morphine+(−)NL ($n = 8$; H: 12.97, $^{*}P < 0.05$), morphine+(+)NL ($n = 5$; $^{*}P < 0.05$) *vs* morphine alone ($n = 7$). **f.** Western blot analysis of P2X4R protein expression in microglia cultures following treatment with morphine (100 nM, $n = 10$ trials, H: 26.49, $^{***}P < 0.001$), morphine+(−)NL ($P > 0.05$), morphine+(+)NL ($n = 5$, $^{***}P < 0.001$), (−)NL ($n = 3$, $P > 0.05$), (+)NL ($n = 6$, $P > 0.05$) *vs*

saline ($n = 10$). **g.** ATP-evoked rise in intracellular [Ca^{2+}] in cultured microglia treated with morphine (100 nM, $n = 54$ cells, H: 67.98, ***$P < 0.001$), morphine+(−)NL ($n = 38$, $P > 0.05$), morphine+(+)NL ($n = 40$,***$P < 0.001$), (−)NL ($n = 15$, $P > 0.05$), (+)NL ($n = 15$, $P > 0.05$), or saline ($n = 35$). **h.** Western blot of P2X4R protein from spinal cords isolated from rats treated for 5 days with intrathecal saline, morphine, morphine+(−)NL, morphine+(+)NL. **i.** ELISA-based measurement of BDNF release from microglia treated with morphine+(−)NL ($n = 5$ trials, H: 14.29, ***$P < 0.001$), morphine+(+)NL ($n = 5$,***$P < 0.001$), *vs* morphine ($n = 14$). **j.** ELISA-based measurement of BDNF release from microglia treated with morphine ($n = 4$ trials, H: 15.84, ***$P < 0.001$), morphine+LPS-RS 1 ng/ml ($n = 4$,***$P < 0.001$), morphine+LPS-RS 10 ng/ml ($n = 4$,***$P < 0.001$), morphine+LPS-RS 100 ng/ml ($n = 4$,***$P < 0.001$), LPS-RS 100 ng/ml ($n = 4$,***$P < 0.001$) *vs* control ($n = 4$). **k**. Effect of morphine (escalating doses from 10 to 40 mg/kg intraperitoneally twice a day for 7 days) on mechanical sensitivity of TLR4 deficient C3H/HeJ mice ($n = 11$) *vs* the wild type C3H/HeOuJ ($n = 8$). Mechanical sensitivity index was calculated as (10-PWs)/PWs (10 = stimulations with 3.41 g calibrated filament; PWs = paw withdrawals). No differences were observed in the development of mechanical allodynia between mice groups (U: 30; $P > 0.05$). All threshold values in the figure are normalized to the baseline. Abb.: PWT = paw withdrawal threshold; CTR = control; MS = morphine sulphate; (−)NL = (−)-naloxone; (+)NL = (+)-naloxone; LPS-RS = lipopolysaccharide from Rhodobacter sphaeroides; i.u.: intensity units; error bars = s.e.m.